Higher-order mode-coupling theory analysis of dielectric measurements on semi-crystalline PET (poly(ethylene terephthalate))

1999 J. Phys.: Condens. Matter 11 8807

(http://iopscience.iop.org/0953-8984/11/45/305)

J. Phys.: Condens. Matter **11** (1999) 8807–8817. Printed in the UK PII: S0953-8984(99)04720-7

Higher-order mode-coupling theory analysis of dielectric measurements on semi-crystalline PET (poly(ethylene terephthalate))

H Eliasson and B-E Mellander

Department of Experimental Physics, School of Physics and Engineering Physics, Göteborg University and Chalmers University of Technology, SE-412 96 Göteborg, Sweden

Received 2 June 1999, in final form 26 August 1999

Abstract. Samples of poly(ethylene terephthalate) with different degrees of crystallinity have been investigated by dielectric spectroscopy in the frequency range 10^{-2}–10^{7} Hz and in the temperature range 60 °C–120 °C. The resulting spectra were evaluated within the A_3-scenario of the mode-coupling theory. Quantitative agreement was found between theory and experiment over a frequency range as large as seven decades in the best case. The scaling laws of the theory were also tested and it was found that they were only partially obeyed. We argue that the reason for this is that the limited temperature range and the effect of the activated hopping processes are not taken into account in the present version of the theory.

1. Introduction

The study of the dynamics of glass-forming liquids and polymers is currently a field of intensive activity due to many interesting and, in many cases, still unexplained phenomena observed in these types of material. Due to the complexity and the absence of long-range order in the systems studied, it is quite difficult to find a theoretical model capable of explaining the majority of the phenomena observed. Consequently, most of the theories developed so far start out from some fairly crude assumption about the systems under study. In contrast, the mode-coupling theory (MCT) originates from the microscopic equations of motion for the particles in the liquid [1]. The basic quantity in this theory is the normalized density autocorrelation function:

$$\phi(q,t) = \frac{\langle \delta n(q,t)\, \delta n^*(q,0)\rangle}{\langle |\delta n(q,0)|^2\rangle} \tag{1}$$

where $n(q,t)$ is the microscopic number density, q the wave-vector modulus, t the time and $\delta n = n - \langle n\rangle$. The angle brackets indicate ensemble averages. From the asymptotic solutions of the MCT equations, glass transition singularities are found. These are bifurcation singularities belonging to the cuspoid family [2, 3]. Close to such singularities and in an intermediate dynamical region called the β-relaxation region, between the initial microscopic decay and the structural α-process, the factorization property

$$\phi(q,t) = f^c(q) + h(q)G(t) \tag{2}$$

is found to hold, where $f^c(q)$ is the value of the non-ergodicity parameter, $f(q) = \phi(q, t \to \infty)$, at the singularity. This result is also valid for any correlation function $\phi_{AB}(q,t)$ of

0953-8984/99/458807+11$30.00

dynamical variables A and B for which there is some overlap with the density. The implication of the above expression is that the time dependence is determined entirely by the function $G(t)$ which yields a universal dynamical scenario. The function $G(t)$ satisfies the equation

$$\frac{\mathrm{i}\delta}{z^2} - \frac{\delta_0}{z} + \delta_1 G(z) + zG^2(z) + (1+\delta_2)\mathrm{LT}[G^2(t)](z) - \gamma_3 z^2 G^3(z) + (\delta_3+\gamma_3)\mathrm{LT}[G^3(t)](z) + \gamma_4 z^3 G^4(z) + (\delta_4+\gamma_4)\mathrm{LT}[G^4(t)](z) + \cdots + (-1)^k \gamma_k z^{k-1} G^k(z) + (\delta_k+\gamma_k)\mathrm{LT}[G^k(t)](z) + \cdots = 0 \tag{3}$$

where the Laplace transform is given by

$$G(z) = \mathrm{LT}[G(t)] = \mathrm{i}\int_0^\infty \mathrm{d}t\ \exp(\mathrm{i}zt)G(t) \tag{4}$$

in which z is a complex frequency. The parameter δ in the first term in equation (3) is the hopping parameter, describing the rate of hopping of particles across potential barriers, to be discussed below. In the present case this parameter is ignored. The above-mentioned glass transition singularities are classified according to the behaviour of the parameters δ_k, as follows: at the singularity, $\delta_0 = \delta_1 = 0$ and if $\delta_2 \neq 0$ an A_2-singularity or Whitney fold is encountered. If also $\delta_2 = 0$ but $\delta_3 \neq 0$ an A_3-singularity or Whitney cusp singularity has been found, and so on [2, 3]. The parameters γ_k are ordinary numbers given by $f(q)$ and the static structure factor. Each of these singularities introduces its own very specific signature in the dynamical behaviour of the systems studied. The A_2-scenario, which is the simplest and most thoroughly studied, predicts a critical temperature, T_c, above which $\phi(q,t)$ shows a two-step decay which can be approximated by the sum of two power laws with exponents $0 < a < \frac{1}{2}$ and $0 < b < 1$ that are related according to

$$\frac{\Gamma^2(1-a)}{\Gamma(1-2a)} = \frac{\Gamma^2(1+b)}{\Gamma(1+2b)} = \lambda \tag{5}$$

where $\Gamma(x)$ is the gamma function and $\lambda = 1 + \delta_2$ is the so-called exponent parameter. For temperatures below T_c, the long-time power law with exponent b will be replaced by a constant plateau having the value $f^c(q)$. In the frequency domain, above T_c, this behaviour corresponds to a minimum in the imaginary part of the generalized susceptibility

$$\chi''(\omega) = \omega\int_0^\infty G(t)\cos(\omega t)\ \mathrm{d}t \tag{6}$$

centred at $(\omega_{\min}, \chi''_{\min})$ and which can be approximated with the interpolation formula

$$\chi''(\omega) = \frac{\chi''_{\min}}{a+b}\left[b\left(\frac{\omega}{\omega_{\min}}\right)^a + a\left(\frac{\omega_{\min}}{\omega}\right)^b\right]. \tag{7}$$

The two parameters $\omega_{\min}$ and $\chi''_{\min}$ are in this scenario predicted to have the following temperature dependence:

$$\omega_{\min} \propto \left|\frac{T_c - T}{T_c}\right|^{1/2a} \tag{8a}$$

$$\chi''_{\min} \propto \left|\frac{T_c - T}{T_c}\right|^{1/2}. \tag{8b}$$

Below T_c, the low-frequency power law is replaced by a white-noise spectrum, $\chi''(\omega) \propto \omega$. The consequence of this is that the structural α-process disappears for temperatures below T_c and this temperature can thus also be referred to as an ideal glass transition temperature. In

real systems, however, the α-peak continues to exist at temperatures below T_c. This situation is taken into account in the MCT by using a non-vanishing parameter δ in equation (3), representing the effect of activated hopping processes on the dynamics of the system. The result of the inclusion of this parameter is to replace the sharp transition at $T = T_c$ with a smooth crossover and as a result the α-peak will still be present for $T < T_c$.

For the higher-order singularities A_k, with $k \geqslant 3$, equation (3) has the solution [4]

$$G(t) = \rho^2 f(y) \tag{9}$$

where $y = \ln(t/t_1)$, $\rho = \left[2\pi^2/3\mu_k(k-2)^2\right]^{1/2(k-2)}$, $\mu_k = -\delta_k$ and t_1 is introduced in order to set the timescale of the initial microscopic decay. In the A_3-case, which is the focus of attention in this paper, the function $f(y)$ is equal to the Weierstrass elliptic function, $\wp(y)$, defined by the elliptic integral

$$y = \int_{\wp}^{\infty} \frac{\mathrm{d}s}{\sqrt{4s^3 - g_2 s - g_3}} \tag{10}$$

in which the separation parameters g_ℓ are given by $g_\ell = 4\delta_{3-\ell}/\mu_3\rho^{2\ell}$.

Since the quantity of interest in the present paper is the dielectric function, the frequency domain behaviour is of particular importance. For the A_3-cusp scenario, the minimum in $\chi''(\omega)$ found in the A_2-scenario will be distorted and for $g_2 = 0$ it will be replaced with a region of flat dielectric loss [5]. The real and imaginary parts of the dielectric function, $\varepsilon(\omega) = \varepsilon'(\omega) - \mathrm{i}\varepsilon''(\omega)$, can in the present case be written as [5]

$$\varepsilon'(\omega) = f_\varepsilon - \varepsilon_c \wp(y; g_2, g_3) \tag{11a}$$

$$\varepsilon''(\omega) = -\frac{\pi}{2}\varepsilon_c \wp'(y; g_2, g_3) \tag{11b}$$

where

$$\wp'(y) = \mathrm{d}\wp/\mathrm{d}y = -\sqrt{4\wp^3(y) - g_2\wp - g_3}$$

and $y = \ln(1/\omega t_1)$. The parameters f_ε and ε_c will be treated as fitting parameters. The function $\wp(y)$ is homogeneous, i.e. $\wp(y; g_2, g_3) = s^2\wp(sy; s^{-4}g_2, s^{-6}g_3)$. This means that by making a suitable choice of the scaling parameter s, in this case $s = |g_3/4|^{1/6}$, the dielectric function can alternatively be expressed as

$$\varepsilon'(\omega) = f_\varepsilon - c'_\xi \wp\left[y/y_\xi; \pm 12(r/4)^{1/3}, \pm 4\right] \tag{12a}$$

$$\varepsilon''(\omega) = -c''_\xi \wp'\left[y/y_\xi; \pm 12(r/4)^{1/3}, \pm 4\right] \tag{12b}$$

where $r = \left|g_2^3/27g_3^2\right|$. If the parameters g_2 and g_3 are considered to be coordinates in a two-dimensional space, a constant r-value will thus define a line along which the solutions in equations (11), (12) are invariant. In such a coordinate system, the material investigated will describe a path when physical control parameters such as temperature and degree of crystallinity are varied. Along a scaling line, the parameters entering equations (12) will have the following temperature dependence [5]:

$$\frac{1}{y_\xi} \propto \left|\frac{T - T_0}{T_0}\right|^{1/6} \tag{13a}$$

$$c'_\xi \propto \left|\frac{T - T_0}{T_0}\right|^{1/3} \tag{13b}$$

$$c''_\xi \propto \left|\frac{T - T_0}{T_0}\right|^{1/2}. \tag{13c}$$

Here, T_0 is the temperature at which the cusp is reached, i.e. when $g_2 = g_3 = 0$. The line $r = 1$ contains the fold singularities and will be crossed by the path taken by the system when $T = T_c$. The testing of these scaling relations is very important for the determination of the validity of the present theory, and such a test is performed by fitting equations (11) to the experimental data, thereby extracting the g_2-, g_3- and r-parameters. Those spectra with similar r-values are thereafter shifted in the horizontal and vertical directions by multiplication with the scaling factors in equations (13) in order to collapse them on top of the calculated master functions in equations (12).

Since it is impossible to analytically evaluate $\wp(y)$, we proceeded by numerically calculating the integral in equation (10) for given values of $\wp$. Since $y = \ln(1/\omega t_1)$, it was in this way possible to generate sets of curves for $\wp[\ln(1/\omega t_1)]$. The dielectric function was then easily obtained from equation (11). To find g_2 and g_3 for each spectrum, we took advantage of the fact that almost every curve measured showed a distinct maximum and minimum. As described elsewhere [5], the extreme values, $\varepsilon''_{\min}$ and $\varepsilon''_{\max}$, of the imaginary part of the dielectric function can then be used to obtain these two parameters, according to

$$g_2 = 3\left[\frac{2}{\pi^2\varepsilon_c^2}(\varepsilon''^2_{\max} - \varepsilon''^2_{\min})\right]^{2/3} \tag{14a}$$

$$g_3 = -\frac{2}{\pi^2\varepsilon_c^2}(\varepsilon''^2_{\max} + \varepsilon''^2_{\min}). \tag{14b}$$

This reduces the number of parameters to vary to two for the imaginary part and three for the real part. The determination of r turns out to be even easier, since by virtue of equations (14*a*), (14*b*) and the relation just below equation (12),

$$r = \left[\frac{\varepsilon''^2_{\max} - \varepsilon''^2_{\min}}{\varepsilon''^2_{\max} + \varepsilon''^2_{\min}}\right]^2. \tag{15}$$

In this paper, dielectric spectra obtained from measurements on poly(ethylene terephthalate) samples with varying degrees of crystallinity were evaluated in terms of the MCT A_3-scenario. The choice of PET as a model system was motivated by the ease of manufacturing samples with varying degree of crystallinity. Because of this, two control parameters are available and it may therefore be possible to map out a large region of the g_2–g_3 parameter space. The A_3-scenario has previously been applied to dielectric spectra of this polymer both in the amorphous [10] and crystalline [5] states. However, in these cases only the temperature was available as a control parameter.

2. Experimental details

Amorphous poly(ethylene terephthalate) films of thickness 0.25 mm were purchased from Goodfellow Incorporated, UK. From these films, discs with diameter 25 mm were punched out. Samples with different degrees of crystallinity were manufactured by annealing at different temperatures and times; see table 1.

The dielectric measurements were performed in the frequency range 10^{-2} Hz–10 MHz using a Schlumberger Solartron 1260 Impedance Gain/Phase Analyzer together with a Chelsea Dielectric Interface for the frequencies between 10^{-2} Hz and 1 kHz, a Hewlett-Packard HP4284A Precision LCR Meter for the range 20 Hz–1 MHz and a Hewlett-Packard HP4285A LCR Meter between 100 kHz and 10 MHz. The disc-formed samples were painted with electrically conducting silver paint and put between two stainless steel electrodes. The temperature was controlled with a Novocontrol Quatro cryosystem, permitting a temperature

Table 1. Degrees of crystallinity and crystallization conditions for the samples used in the present study.

Sample No	Degree of crystallinity (%)	Annealing temperature and time
1	9	100 °C, 4 h
2	15	100 °C, 7 h
3	26	100 °C, 11 h
4	31	120 °C, 24 h
5	35	160 °C, 24 h

accuracy of within ± 0.1 °C and the sample temperature was measured with a Pt100 resistance thermometer.

To determine the degree of crystallinity of the samples, differential scanning calorimetry (DSC) measurements were performed with a Mettler DSC 30 Low Temperature Cell. The degree of crystallinity was estimated by comparing the areas of the peaks due to recrystallization and melting normalized to the heat-of-fusion value of 124 J g^{-1} corresponding to 100% crystallinity found in the literature [6].

3. Results

Dielectric measurements on PET reveal two relaxation peaks, the lower-frequency α-peak and the secondary β-peak, seen at higher frequencies [15]. The α-peak is the manifestation of the structural relaxation, the freezing in of which leads to the liquid–glass transition. The β-peak can in this case not be explained in terms of side-group motions and is therefore believed to be of the same origin as the so-called Johari–Goldstein processes [11–14]. The results of the curve fits to equations (11) are presented in figures 1 and 2 for two of the samples investigated. To avoid clutter, the curves are truncated at low frequencies where deviations between theory and experiment start to appear. The fitting parameters f_ε, ε_c and t_1 should ideally be temperature independent, but some drift might be expected [5]. In the present case, f_ε and ε_c were found to increase with increasing temperature while t_1 was decreasing. The timescale t_1 was determined to be in the range from 10^{-11} to 10^{-10} s. The differences between the real and imaginary parts as regards the agreement between theory and experiment are probably due to the theoretical expressions for the dielectric function being asymptotic solutions and the Kramers–Kronig relations therefore not being expected to be exactly valid. For sample 2, which has the lower degree of crystallinity, agreement is found between theory and experiment over a frequency range larger than seven decades. In this case, the theory is able to describe a large part of the α-peak. This may be expected since the asymptotic solutions to the MCT include the high-frequency part of the α-peak, which overlaps with the low-frequency part of the β-region. Due to the slow variation of this decay in the time domain in the A_3-case, this overlap extends to longer times or lower frequencies in comparison with the A_2-scenario. For sample 4 (figure 2), the low-frequency spectra do not show as good an agreement between theory and experiment as those for sample 2. One reason for this may be the influence of higher-order scenarios, i.e. A_4. The imaginary part of the dielectric function for this sample does show more 'cusp-like' features, especially at the highest temperature where an almost horizontal plateau is seen. It is therefore possible that we have here an A_3-cusp within an A_4-relaxation scenario. In figure 3 it is clearly seen that the distance to the cusp singularity located at $(g_2, g_3) = (0, 0)$ is decreasing with increasing degree of crystallinity.

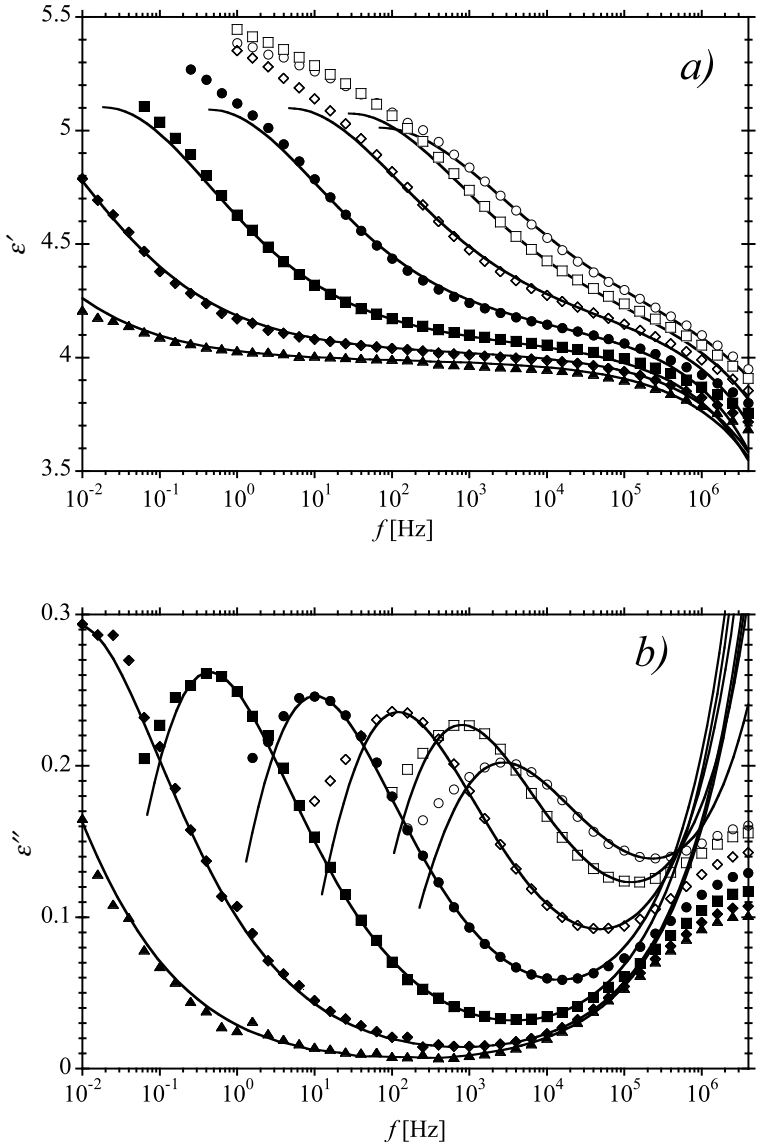

Figure 1. (a) The real part and (b) the imaginary part of the dielectric function for sample 2. Filled triangles: 70 °C; filled diamonds: 75 °C; filled squares: 80 °C; filled circles: 85 °C; open diamonds: 90 °C; open squares: 95 °C; open circles: 100 °C. Full lines are fits to equation (11).

For all samples, the points obtained move from left to right with decreasing temperature. As can be seen from this figure, some of the measured spectra do indeed follow common scaling lines. Since the cusp temperature, T_0, is predicted to be lower than T_c, previously determined to be around 82 °C [10, 16–18], spectra at low temperatures are especially interesting. However, the glass transition temperature is located at around 67 °C for the amorphous sample and is increasing with increasing degree of crystallinity, and this sets a practical low-temperature limit at around 70 °C for the measurements since the lowest frequency measured was 10^{-2} Hz.

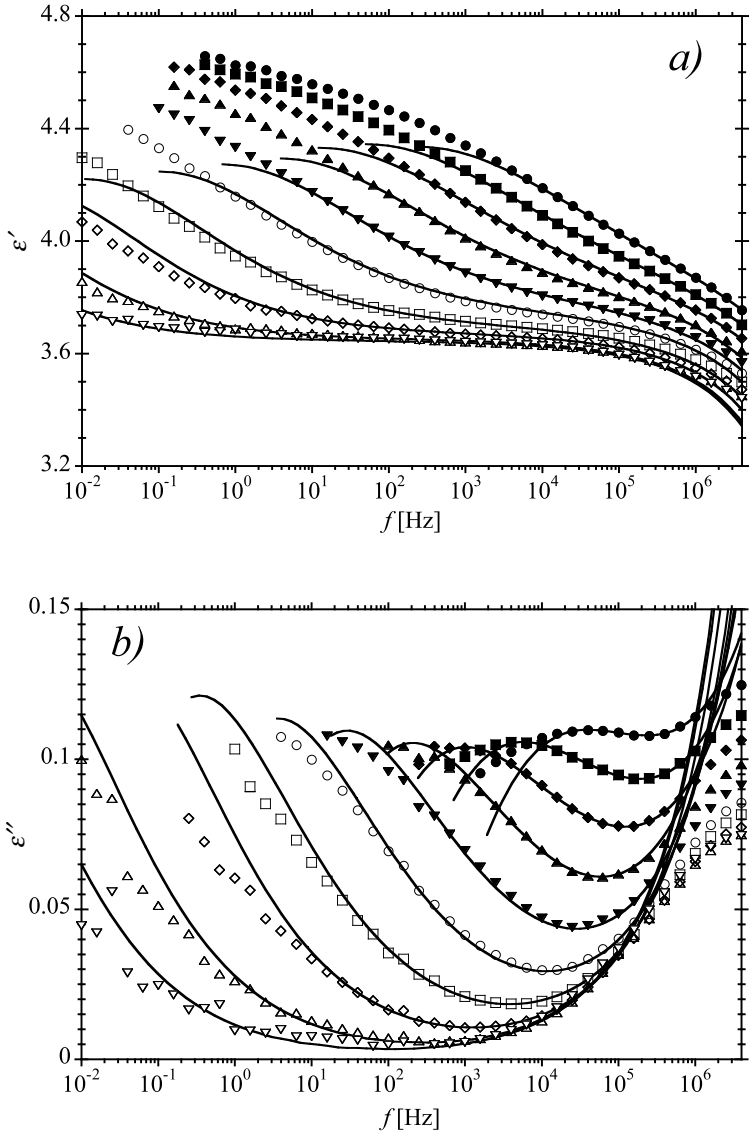

Figure 2. (a) The real part and (b) the imaginary part of the dielectric function for sample 4. Open down-pointing triangles: 70 °C; open up-pointing triangles: 75 °C; open diamonds: 80 °C; open squares: 85 °C; open circles: 90 °C; filled down-pointing triangles: 95 °C; filled up-pointing triangles: 100 °C; filled diamonds: 105 °C; filled squares: 110 °C; filled circles: 115 °C. Full lines are fits to equation (11).

In figure 4, the rescaled imaginary parts of $\varepsilon(\omega)$ corresponding to the data points along the scaling line $r = 0.90$ are plotted together with the predicted master curve, given by equation (12*b*). The calculated r-values for these curves were within the range 0.90 ± 0.04. Even such relatively small deviations produce a rather large scatter and this might be why especially c''_ξ in figure 5 shows quite large fluctuations around a constant value. The timescale y_ξ in the same graph is also more or less constant but has less scatter. It is thus not possible to

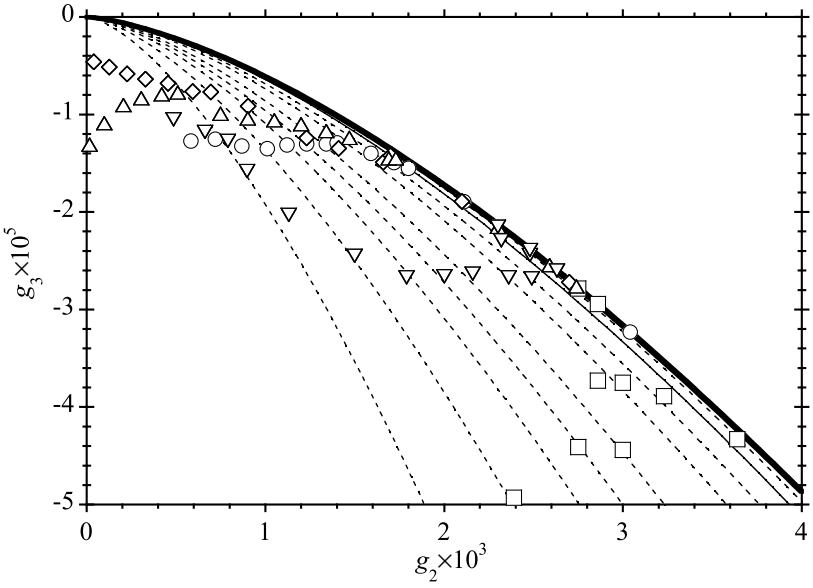

Figure 3. The parameter space defined by the two separation parameters g_2 and g_3. The symbols represent the five samples. Squares: sample 1; down-pointing triangles: sample 2; circles: sample 3; up-pointing triangles: sample 4; diamonds: sample 5. The thick full line is the fold line. Dashed lines are scaling lines for $r = 0.10$, 0.20, 0.31, 0.40, 0.50, 0.68, 0.79 and 0.96, from left to right. The thin full line is the scaling line for $r = 0.90$; see the text.

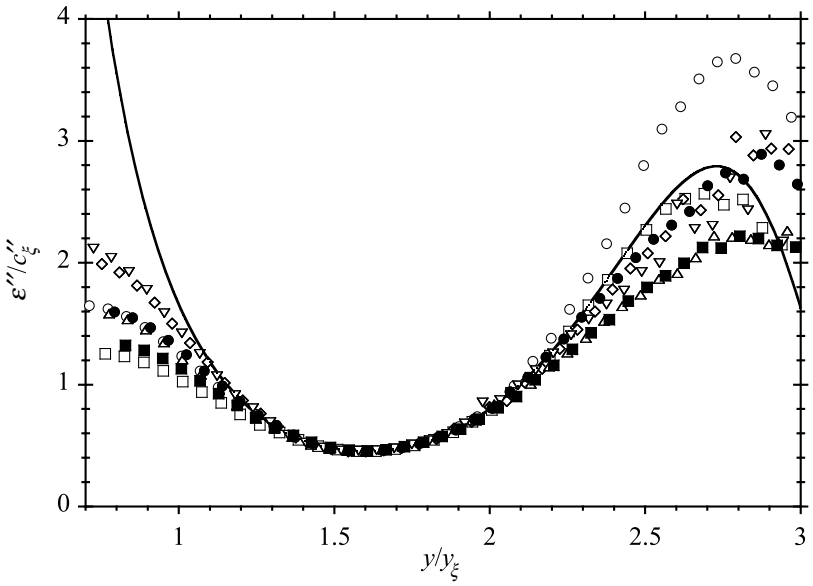

Figure 4. Rescaled spectra along the scaling line $r = 0.90$. Open circles: sample 2, 80 °C; open squares: sample 2, 83 °C; filled circles: sample 3, 86 °C; filled squares: sample 3, 88 °C; open diamonds: sample 4, 85 °C; open up-pointing triangles: sample 4, 88 °C; open down-pointing triangles: sample 5, 80 °C. The full line is the master curve calculated from equation (12*b*).

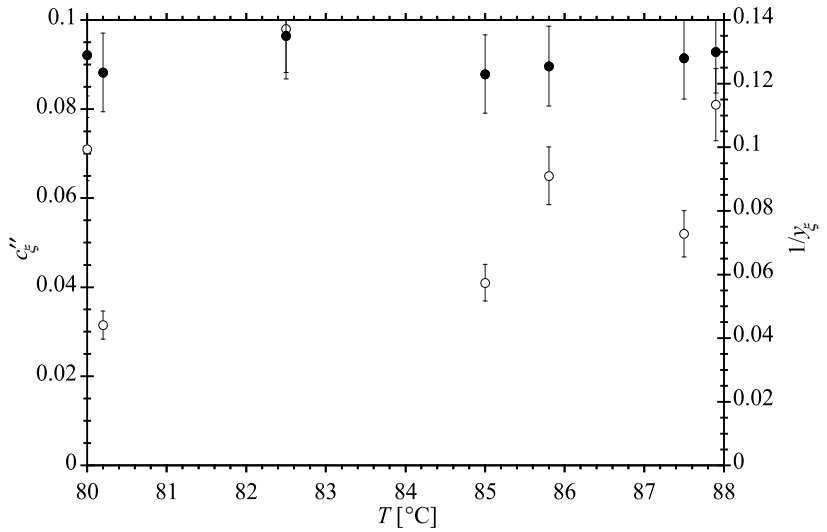

Figure 5. Scaling parameters extracted from figure 4. Open circles: c''_ξ; filled circles: $1/y_\xi$.

test the scaling-law predictions of equations (13) in this case.

Even for the A_3-scenario the minimum in $\varepsilon''(\omega)$ should follow a square-root law as in equation (8*b*). This is tested in figure 6. Above T_c, a plot of ε''^2 should yield a straight line which is zero at $T = T_c$. The deviations from the straight line seen in figure 6 at temperatures close to and below T_c are attributed to activated hopping processes not included in the idealized theory which serve to smooth out the sharp transition at T_c. The values of T_c produced from this analysis are presented in table 2.

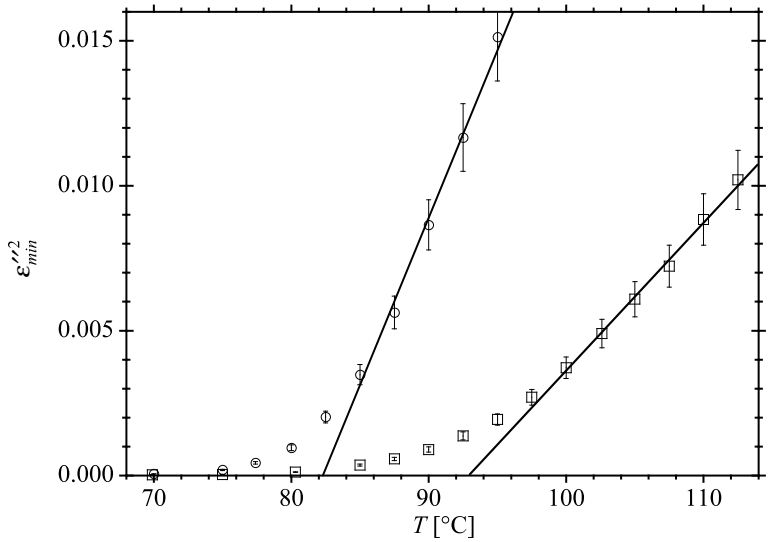

Figure 6. The squares of the values of $\varepsilon''(\omega)$ at the minimum as functions of temperature for samples 2 (circles) and 4 (squares). The full lines are the best fits to straight lines, yielding $T_c = 82 \pm 2\ ^\circ$C for sample 2 and $T_c = 93 \pm 2\ ^\circ$C for sample 4.

Table 2. Values of the critical temperature T_c for the different PET samples.

Sample No	T_c (°C)
1	82 ± 2
2	82 ± 2
3	88 ± 2
4	93 ± 2
5	88 ± 2

4. Discussion

The higher-order glass transition scenarios of the MCT have to date almost exclusively been observed in dielectric measurements on polymers [5, 8–10]. A cusp scenario has however recently also been identified in model calculations for a sticky hard-sphere system [7]. One may argue that the MCT is not applicable to complex systems like PET. It is however important to realize that the expressions (11), (12) for the dielectric function and also the scaling predictions of equations (13) are not dependent on the detailed microscopic structure of the system studied, provided that one can drive it close enough to a singularity [1, 4, 5]. This implies a universal dynamical scenario for this class of materials. Accordingly, any microscopic theory for polymer dynamics developed out of a mode-coupling theory will incorporate these scenarios [19, 20]. This is the justification for applying the MCT to polymeric systems such as PET. It may be noted that a fairly recent dielectric study of amorphous PET did seem to corroborate the idea that the MCT is not applicable to PET [17, 18]. A further analysis of the same data showed, however, that the MCT is also applicable in this case [10].

The scaling laws in equations (13) were not obeyed in the present study by the data obtained from our measurements. There might be many reasons for this situation arising. For example, the cusp temperature, T_0, could be lower than expected, meaning that the measurements should have been performed at even lower temperatures, and consequently also lower frequencies, in order to see the entire minimum. In the present case, the limited sensitivity of the instruments used combined with the low loss of the samples restricted the frequency range at lower frequencies. The fits might also be disturbed by the presence of activated hopping processes, which is evident from the fact that the α-peak is still present for $T < T_c$ and also from figure 3, where for temperatures below T_c, the g_2- and g_3-parameters are still located on the left-hand side of the fold line. This means that the spectra for which $T < T_c$ might have been fitted to a curve actually representing $T > T_c$ in the idealized theory. The inclusion of a non-vanishing hopping parameter in the MCT equations may modify the values of g_2 and g_3 close to the fold line with the result that better results are produced. At present, however, equation (3) has not been solved for $k = 3$ and $\delta \neq 0$.

For the higher-order singularities A_k, $k \geqslant 3$, the scaling law in equation (8*b*) should still apply [5]. This is demonstrated in figure 6 for samples No 2 and No 4. Clearly, the data for both of these samples are in agreement with this prediction for $T > T_c$. The differences in the value of T_c between the samples—see table 2—are due to the fact that the paths taken by the different systems in the g_2–g_3 parameter plane are crossing the fold line at different locations; see figure 3. When moving along the fold line towards the cusp point at $(g_2, g_3) = (0, 0)$, the critical temperature T_c will decrease and it will become equal to T_0 at the cusp point. Since the sample with the highest degree of crystallinity has the path closest to the cusp point, one would expect this to produce the lowest value of T_c. As seen in table 2, this is not the case, and the reason for this discrepancy might also in this case be that, close to the fold line, activated hopping processes play an important role and this will change the direction of the path causing

it to cross the fold line at some other point.

In summary, we find that the MCT A_3-scenario is capable of describing the dielectric data obtained for PET with a varying degree of crystallinity. The scaling laws in equations (13) predicted for this scenario were however not obeyed and we suggest this to be either due to the effect of activated hopping processes or because the cusp temperature T_0 was lower than expected.

Acknowledgments

The authors would like to express their gratitude to Professor Alois Loidl, Dr Peter Lunkenheimer, Ulrich Schneider and Robert Brand at Experimentalphysik V, Universität Augsburg, Augsburg, Germany, for their hospitality and generous support. We are also grateful to Dr Lennart Sjögren for valuable comments on the manuscript. This work received financial support from the Swedish Natural Science Research Council and Stiftelsen Anna Ahrenbergs fond.

References

[1] For a review of the MCT, see e.g.
Götze W 1991 *Liquids, Freezing and Glass Transition* ed J-P Hansen, D Levesque and J Zinn-Justin (Amsterdam: North-Holland)
Götze W and Sjögren L 1992 *Rep. Prog. Phys.* **55** 241
[2] Arnol'd V I 1986 *Catastrophe Theory* 2nd edn (Berlin: Springer)
[3] Gilmore R 1981 *Catastrophe Theory for Scientists and Engineers* (New York: Wiley)
[4] Götze W and Sjögren L 1989 *J. Phys.: Condens. Matter* **1** 4203
[5] Sjögren L 1991 *J. Phys.: Condens. Matter* **3** 5023
[6] Coburn J C and Boyd R H 1986 *Macromolecules* **19** 2238
[7] Fabbian L, Götze W, Sciortino F, Tartaglia P and Thiery F 1999 *Phys. Rev.* E **59** R1347
[8] Flach S, Götze W and Sjögren L 1992 *Z. Phys.* B **87** 29
[9] Halalay I 1996 *J. Phys.: Condens. Matter* **8** 6157
[10] Eliasson H, Mellander B-E and Sjögren L 1998 *J. Non-Cryst. Solids* **235–237** 101
[11] Goldstein M 1969 *J. Chem. Phys.* **51** 3728
[12] Johari G P and Goldstein M 1970 *J. Chem. Phys.* **53** 2372
[13] Johari G P and Goldstein M 1971 *J. Chem. Phys.* **53** 4245
[14] Johari G P 1973 *J. Chem. Phys.* **58** 1766
[15] McCrum N G, Read B E and Williams G 1991 *Anelastic and Dielectric Effects in Polymeric Solids* (New York: Dover)
[16] Sjögren L 1990 *Basic Features of the Glassy State* ed J Colmenero and A Alegria (Singapore: World Scientific) p 137
[17] Hofmann A, Kremer F and Fischer E W 1993 *Physica* A **201** 106
[18] Hofmann A, Kremer F and Schönhals A 1994 *Disorder Effects on Relaxational Processes* ed R Richert and A Blumen (Berlin: Springer) p 309
[19] Rostiashvili V G 1990 *Sov. Phys.–JETP* **70** 563
[20] Rostiashvili V G 1992 *Physica* A **182** 557